ORIGINAL RESEARCH REPORT

In vitro and in vivo evaluation of a novel bioresorbable magnesium scaffold with different surface modifications

Roman Menze[1] | Eric Wittchow[2]

[1]MeKo Laser Material Processing e.K, Sarstedt, Germany

[2]CVPath Institute, Inc., Gaithersburg, Maryland

Correspondence
Roman Menze, Dipl.-Ing., Im Kirchenfelde 12-14, 31157 Sarstedt, Germany.
Email: menze@meko.de

Abstract

The novel Resoloy® rare earth magnesium alloy was developed for bioresorbable vascular implant application, as an alternative to the WE43 used in Biotronik's Magmaris scaffold, which received CE approval in 2016. Initially, the Magmaris showed very promising preclinical and clinical results, but the formation of an unexpected conversion product and a too fast loss of integrity has proven to be a flaw. The safety and efficacy of Resoloy, which is intended to be bioresorbed without any remnants, has been investigated in an in vitro degradation study and a porcine coronary animal model. Four different groups of scaffolds composed of Resoloy (Res) as the backbone material and additionally equipped with a fluoride passivation layer (Res-F), a polyester topcoat (Res-P), or a duplex layer composed of a fluoride passivation layer and a polymeric topcoat (Res-PF) were compared to a Magmaris scaffold in an in vitro degradation test. Preclinical safety and efficacy of Res-F and Res-PF were subsequently evaluated in a coronary porcine model for 12 and 28 days. Scanning electron microscope, quantitative coronary angiography, micro-computed tomography, histopathology, and histomorphometry analyses were conducted to evaluate preclinical parameters and degradation behavior of the scaffolds. Res-PF with a duplex layer shows the slowest degradation and the longest supporting force of all test groups. The in vitro data are confirmed by the results of the in vivo study, in which Res-PF exhibited a longer supporting force than Res-F, but also caused higher neointima formation. Both studied groups showed excellent biocompatibility. A starter colonization of the strut area with cells during bioresorption was observed. The in vitro degradation test shows that a combination of MgF_2 passivation and a PLLA topcoat on a Resoloy magnesium backbone (Res-PF) leads to a much slower degradation and a longer support time than a Magmaris control group. In a preclinical study, the safety and efficacy of this duplex layer could be demonstrated. The beginning colonization of the degraded strut area by macrophages can be seen as clear indications that the resorption of the intermediate degradation product takes a different course than that of the Magmaris scaffold.

1 | INTRODUCTION

Second generation drug eluting stents (DES) have proven safety and efficacy in clinical trials and have shown a reduced risk of revascularization and a lower risk of definitive stent thrombosis when compared to bare metal stents.[1]

However, there are some remaining limitations, such as, stent thrombosis (ST), neoatherosclerosis and adverse effects on vasomotion resulting in rising adverse events over time.[2,3]

To overcome these limitations, bioresorbable scaffolds (BRS) were introduced. Firstly, generation BRS were based on polymers and showed promising but not satisfying clinical results due to scaffold thrombosis and higher rates of major adverse cardiac events compared to Everolimus eluting stents.[4]

A potential improvement due to better mechanical properties could be a resorbable metallic scaffold, the first representative of which was the Magmaris from Biotronik, which received CE approval in 2016. The Magmaris scaffold consists of a magnesium rare earth alloy (refined WE43) as the backbone and a limus-eluting poly-L-lactide (PLLA) coating. Preclinical and clinical studies revealed safety, efficacy, and favorable rates of ST for magnesium-based scaffolds.[5-9]

Recent, long-term studies uncovered one drawback of the Magmaris: The scaffold is not completely disappearing, but is replaced over time by a translucent endogenous material which was seen in histology as well as in optical coherence tomography (OCT) and intravascular ultrasound up to 730d.[7,8,10] Although no adverse effect of the conversion product has been reported, the biological long-term effect is unknown.[11]

Resoloy was therefore developed as an alternative to WE43, which is used as backbone material in the Magmaris. Preliminary tests gave rise to the hope that Resoloy would be completely bioresorbed without leaving a long-lasting transformation product in the tissue, while the mechanical properties also slightly outperform those of WE43 (Table 1).

At present, despite all technical progress in alloy development, there is no magnesium alloy known, which has a degradation rate slow enough to guarantee the clinically-relevant 3 month support time preferred for a coronary implant.[9,11] Therefore, the Resoloy scaffolds (Res) of the current study were equipped with a fluoride-based passivation layer (Res-F) in one version, and with a PLLA coating (Res-P) in a second version and a combination of both, fluoride and PLLA on the top of the passivation layer (Res-PF) to seal spatial defects[12,13] in a third version.

In this article, the in vitro degradation rate and loss of radial strength over time of the bare Resoloy scaffold was compared to three other surface modifications as well as to the Magmaris scaffold. In addition, a preclinical study with the Res-F and Res-PF surface modification of the Resoloy scaffold over 12 and 28 days was designed to collect information about feasibility, safety and resorption in a coronary porcine model and to help arrive at a risk benefit assessment for the two surface modifications.

2 | MATERIAL AND METHODS

The Res scaffolds were produced of Resoloy (MeKo, Sarstedt, Germany), which is a rare earth element magnesium alloy based on the Mg-Dy system. In contrast to the alloy used for the Magmaris, Resoloy is free of yttrium and gadolinium. All tested Resoloy scaffold groups refer to bioresorbable metal scaffolds consisting of a balloon-expandable delivery system carrying a 3.0 × 15 mm scaffold with an eight-crown four-link design and nearly square-shaped struts at a width and thickness of 140/130 μm, modified with the correspondent passivation and coating mentioned before. The Res-F refers to a bioresorbable metal scaffold modified with a magnesium fluoride (MgF_2) passivation layer. The Res-P refers to the Res scaffolds but with a PLLA coating and the Res-PF refers to the Res scaffolds with a duplex layer of MgF2 with an additional PLLA coating on top.

The Magmaris bioabsorbable magnesium scaffold has a sirolimus-eluting bioresorbable PLLA coating with a sirolimus load of 1.4 μg/mm² using a 3.0 × 15 mm scaffold with a 150 μm strut thickness (Magmaris; Biotronik AG, Buelach, Switzerland).

2.1 | Surface characterization

In order to assess integrity of the surface modifications after crimping to ∼Φ1.0 mm on a balloon-expandable delivery system, followed by expansion to ∼Φ3.3 mm, the surfaces of the scaffolds were observed with a scanning electronic microscope (TeScan Vega III, Czech Republic). The surface was coated with a thin layer of gold for better conductivity by a sputter coater (Cressington Sputter Coater 108auto, UK).

TABLE 1 Alloying elements in wt.% and mechanical properties of Resoloy and WE43[25-27]

Alloying elements [wt.-%]	Resoloy	WE43
	Mg: balance	Mg: balance
	Zn: 0.75	Zn: —
	Zr: 0.3	Zr: —
	Y: —	Y: 4.0
	Rare earth elements:	Rare earth elements:
	Dy: 8	Dy: 0.5
	Nd: 0.75	Nd: 2.0
	Gd: —	Gd: 0.5
Ultimate tensile strength	>270 MPa	∼260 MPa
Elongation to failure	>23%	∼18%

The thickness of the fluoride layer was measured by element mapping of a linescan on cross sections of Res-F scaffolds (EDX, Fisher Scientific). To measure the thickness of the polymer coating, cross sections of Res-PF were visualised using a confocal laser scanning microscope (Keyence VK-X 150, Japan). If necessary, the contrast of the images was enhanced (Adobe Photoshop CC) to better recognize details.

2.2 | In vitro degradation test

A degradation tester was developed to simulate physiological conditions encountered in in vivo vessels. The details of the in vitro degradation tester and the test setup will be described elsewhere (Menze et al manuscript in preparation). Briefly, the custom-made degradation tester for magnesium alloy scaffolds is shown in Figure 1.

It consisted of a test channel with a camera system, a peristaltic pump, and a fluid reservoir. The test channels were made from silicone tubing with an inner diameter of 2.8 mm and an intended compliance comparable to the human artery. The actual compliance was measured by mounting the tube horizontally between two tube fittings and applying an internal pressure using a pressure regulator (SMC, Switzerland) with a range from 0–1 bar. While the pressure was increased incrementally, the exact tube internal pressure was measured with a pressure sensor (ifm, Germany). At the same time, the subsequent increase of the tube diameter was measured with a triple-axis laser micrometer (Laserlinc). The normalized compliance was calculated as the ratio between variations in cross-sectional tube

diameter and applied pressure, according to the following equation for equal lengths of the tubes[14]:

$$C = \frac{\Delta D}{\Delta P * D_0} \tag{1}$$

500 ml of phosphate-buffered saline (PBS) with a pH value of 7.40 ± 0.25 prior to the test was used for each scaffold. The degradation tester was set to 37°C. The magnesium ion concentration, the pH value of the medium and the diameter of the tube were each recorded periodically. The tube diameter is directly proportional to the loss of radial strength of the scaffolds and is used as a surrogate for it, as serial non-destructive measurements are not possible. The scaffolds were mounted onto an angioplasty balloon (∼Φ1.0 mm), which was then dilated with 14–16 bar in the test tube in front of a camera system to achieve an outer diameter of the scaffold of 3.1–3.2 mm causing a 10% minimum overstretch of the test tube. Due to the different design of the Resoloy-based scaffolds versus the Magmaris, the Mg ion concentration in the degradation test is expressed per [mm²], to account for the difference in surface areas.

2.3 | Coronary porcine study

The in vivo testing was conducted at a contract research organization (AccelLAB Inc., Boisbriand, Canada) using a porcine coronary artery model. The evaluation compared quantitative coronary angiography (QCA), histomorphometry, histopathology data, and micro-computed tomography (μ-CT) of Res-F- and Res-PF. The study protocol was approved by the Institutional Animal Care and Use Committee of the testing facility and was in compliance with the Canadian Council on Animal Care regulations.

2.3.1 | Implantation

A total of 12 Res-F and Res-PF scaffolds were implanted into the coronary arteries of 6 juvenile Yucatan mini swine with a weight of 37.2–41.7 kg. Animal husbandry, medication administration, and scaffold implantation were performed according to standards as previously reported.[9] Segments of the main coronary arteries RCA and LAD with favourable anatomy and diameter were selected by angiography at the discretion of the interventionalist and the devices were implanted targeting a balloon-to-artery ratio of 1.1 to 1.2. Vessel sections were harvested at 12 days and 28 (±1) days. The tissue processing was performed according to a procedure specially adapted for magnesium implants.[15]

2.3.2 | QCA and histomorphometry

QCA and histomorphometry analyses were performed as previously published by Wittchow et al.[9] QCA was conducted using Medis QAngio® XA 7.3 software (Medis, Leiden, the Netherlands).
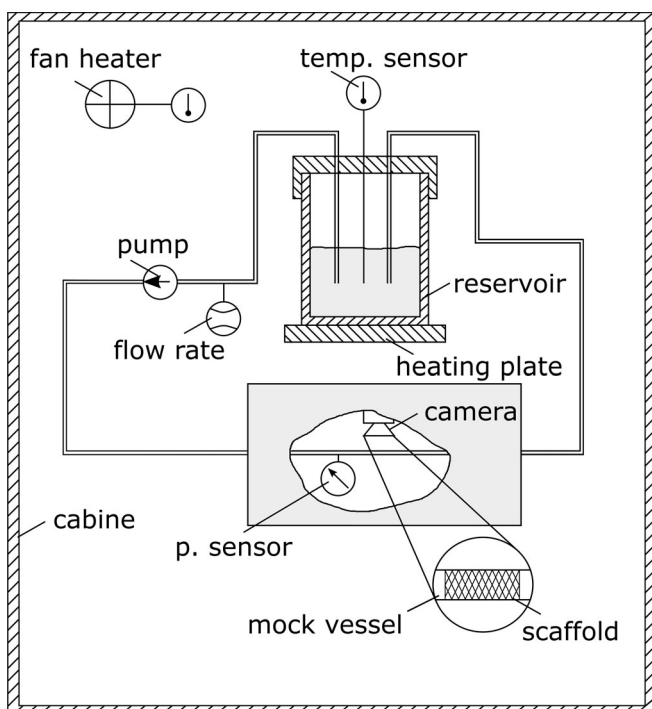

FIGURE 1 In vitro degradation test setup

2.3.3 | Histopathology

For the histological analysis by light microscopy with image capture, ~8 μm thick histological sections of the proximal, middle, and distal segments of the stented artery were stained with haematoxylin-eosin (HE) and elastin trichrome (ET). morphometry was performed using Image Pro Premier 9.2 (Media Cybernetics Inc., Rockville, MD).

2.3.4 | Qualitative backbone analysis

After embedding in poly(methyl methacrylate), high-resolution μ-CT scans (Nikon XT H 225 with a resolution of 1.5–3.0 μm/voxel; Nikon, Tokyo, Japan) were performed for all samples.

2.4 | Statistical analysis

All scores were determined as mean ± standard deviation (SD) of the section means unless stated otherwise. Equal variance and normality tests were performed, and if they failed, a Mann–Whitney Rank Sum test was performed. When equal variance and normality were observed, a t test was performed. A p-value <0.05 was considered statistically significant.

3 | RESULTS

3.1 | Surface characterization

Figure 2a shows the surface of the Res-F and Figure 2b shows a representative abluminal strut-side of the Res-F after crimping and dilating with a balloon catheter. An EDX linescan showed that this MgF2 layer has a thickness of about 1-2 μm. The coating remained unchanged in the neutral axis, where no deformation occurred. At the deformed radii, the coating appeared brittle and flaky. In contrast, the polymeric top coating of the Res-PF in Figure 2c had a homogenous, pinhole-free appearance and showed no cracks even after crimping and dilation. Coating delamination,[16] which was reported for a select number of commercial DES in areas of high deformation after expansion of the stent, was not observed in this study
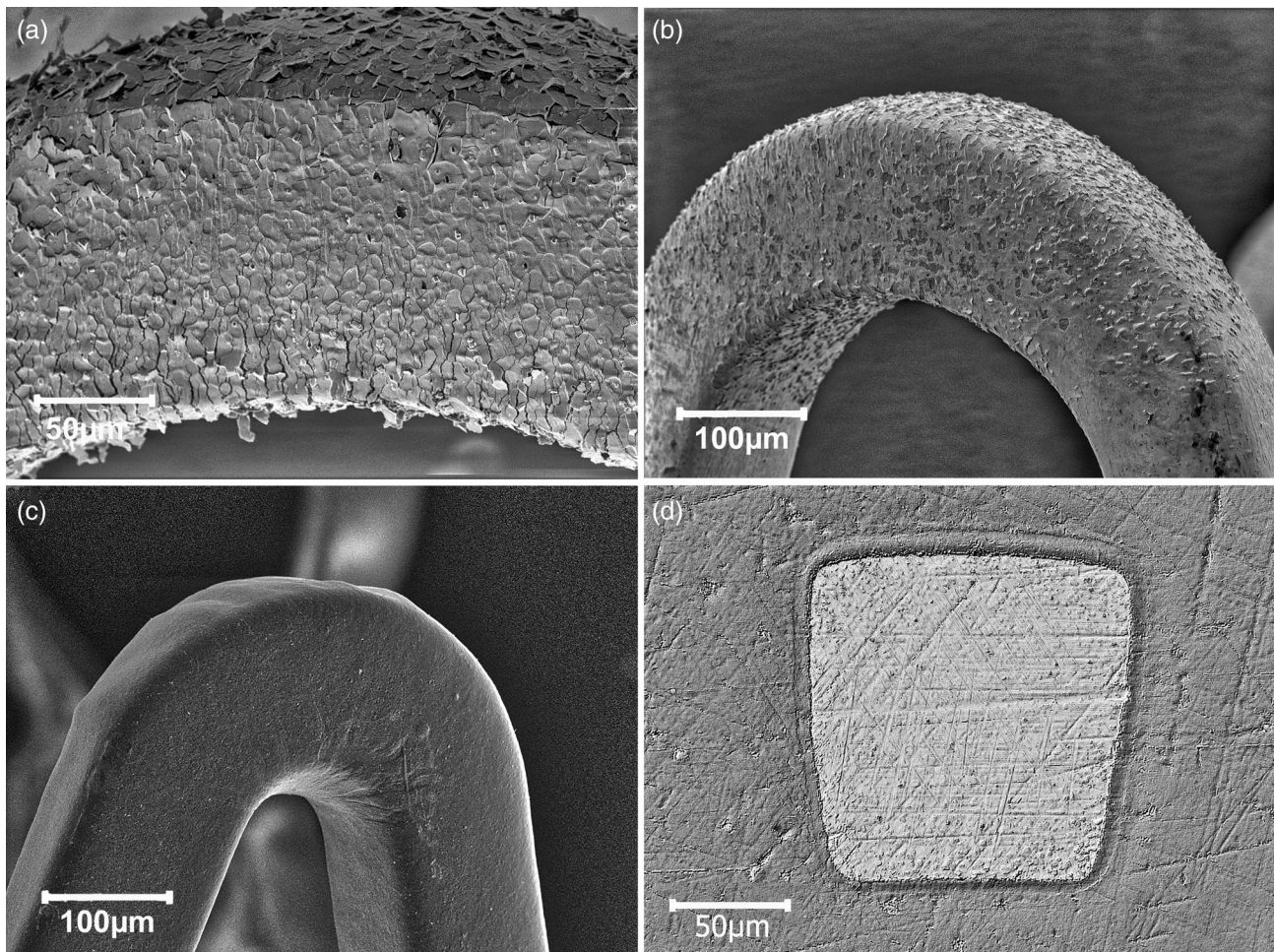

FIGURE 2 SEM images of Res-F before (a) and after crimping and dilating (b), RES-PF after crimping and dilating (c), cross section of Res-PF (d)

The cross section in Figure 2d of the Res-PF showed a homogenous polyester coating with an approximately 5 μm thickness on the luminal side and 9 μm on the abluminal side.

3.2 | In vitro degradation test

The results of mean magnesium release in PBS are provided in Figure 3. It can be seen that the increase in Mg concentration appeared to be linear for all groups and the curve only flattened when more than approximately 80% of the magnesium alloy degraded. The bare Res scaffold without any surface modification exhibited the fastest corrosion, followed by the Res-F group and the Mag. The Res-P degraded more than 10× slower than the corresponding Res and 5× slower than the Mag. The Res-PF group had the slowest degradation of all five test groups, which can be visually observed in Figure 4.

The test tube's compliance was with $5\% \times \text{mmHg}^{-1} \times 10^{-2}$ in the range as reported for human arteries-approximately $5–10\% \times \text{mmHg}^{-1} \times 10^{-2}$.[17,18] Figure 5 shows the relationship between tube diameter and applied internal pressure during compliance measurement, allowing conclusions to be drawn about the remaining radial strength of the stent during the degradation test.

The test tubes equipped with Res or Res-F, respectively lost any implant-induced overstretch after 3–4 days and returned stepwise to their original inner diameter of 2.8 mm. The loss of radial force over time is depicted in Figure 6. The Mag reached this point by day 15, whereas the Res-P was able to resist the external force of the test tube for 40 days, and the Res-PF for more than 50 days.

In Figure 7, the reduction in test tube overstretch in relation to the concentration of Mg^{2+} is shown. The former directly correlates to radial strength of the scaffold, while the latter signifies the process of degradation. For the bare Res, the reduction of test tube diameter was directly proportional to scaffold degradation, whereas the polymer-coated scaffolds (Res-P, Res-PF, and Mag) lost comparable test tube overstretch but at lower Mg^{2+} release, although the figure does not show that the overall process happened over a much longer time frame (in the case of the polymer-coated scaffolds).

3.3 | Coronary porcine study

3.3.1 | Device acute performance, QCA, histopathology, and histomorphometry

All 12 scaffolds of Res-F and Res-PF were implanted successfully in the RCA and LAD. No animal died before scheduled euthanasia. The mean balloon to artery ratio (oversize) ranged from 1.11 ± 0.04 to 1.15 ± 0.03, with no significant difference between the test groups (Table 2). QCA showed a LLL at 12 days which was significantly lower in Res-F (0.04 ± 0.11) than in Res-PF (0.28 ± 0.18, p = 0.01), and was similar after 28 days (0.57 ± 0.22 and 0.41 ± 0.20, p = 0.41).

Histomorphometry analyses revealed similar external elastic lamina (EEL) area, medial and luminal area for both groups at each time point (Table 2). The neointimal area appeared to be slightly higher in Res-PF than in Res-F at both time points (0.96 ± 0.15 vs. 1.36 ± 0.30, p = 0.11 and 1.55 ± 0.62 vs. 2.22 ± 0.35, p = 0.18).

The inflammation scores were moderate in both groups at both time points (1.34 ± 0.36 vs. 1.75 ± 0.17, p = 0.15, and 1.29 ± 0.07 vs. 1.26 ± 0.21, p = 0.81). After 12 days though, it appeared slightly higher in Res-PF than in Res-F. The fibrin scores in Res-F were low at 12 days (0.74 ± 0.33) and very low at 28 days (0.13 ± 0.07), while the moderate fibrin score of Res-PF after 12 days (1.47 ± 0.40) diminished to a low score at 28 days (0.28 ± 0.09).

After 12 days, the inflammation predominantly consisted of mixed inflammatory infiltrates (macrophages, multinucleate giant cells [MGCs], eosinophils, neutrophils, lymphocytes), while after 28 days it predominantly consisted of macrophages and MGCs in all treated arteries without occurrence of any granuloma.

3.3.2 | Micro-computed tomography analysis

The μ-CT images show full expansion for all scaffolds. A representative picture is depicted in Figure 8d. Single strut breakages were seen in both groups at 28 days. Res-F showed strut breakages on ring segments and connectors, while Res-PF scaffolds exhibited few fractures overall. Those existing were mainly in the connectors.
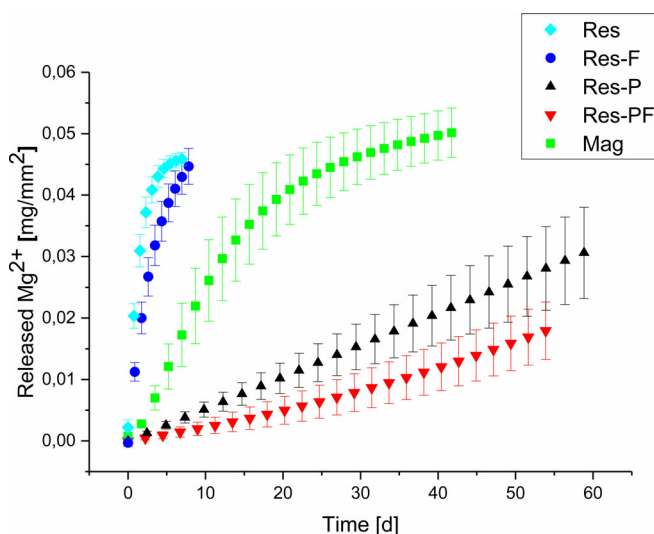
4 | DISCUSSION

This study has shown that Resoloy exhibits the necessary mechanical properties to produce a bioresorbable balloon-expandable scaffold, which can be crimped and dilated safely.
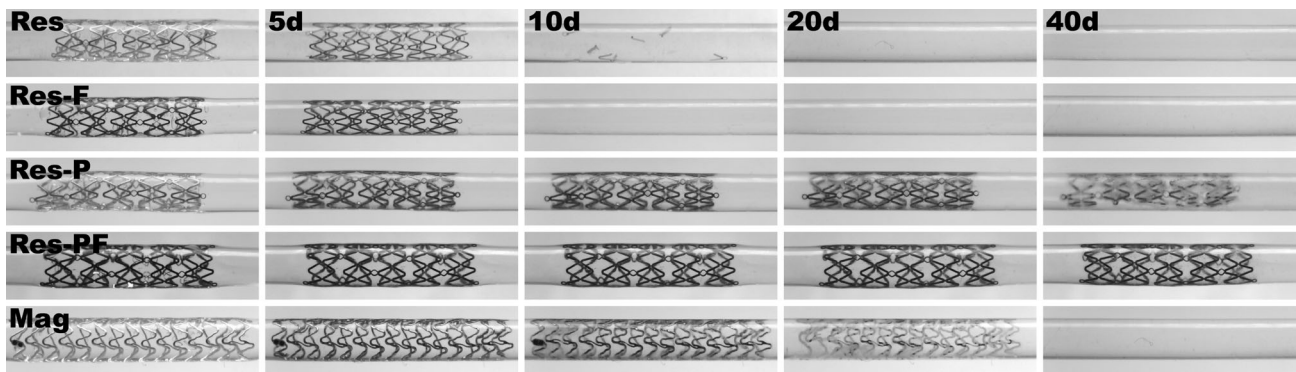

FIGURE 3 Released Mg^{2+} [mg/mm^2] per time [d] of Res (n = 7), Res-F (n = 5), Res-P (n = 4), Res-PF (n = 5), and Mag (n = 4) in the degradation test setup

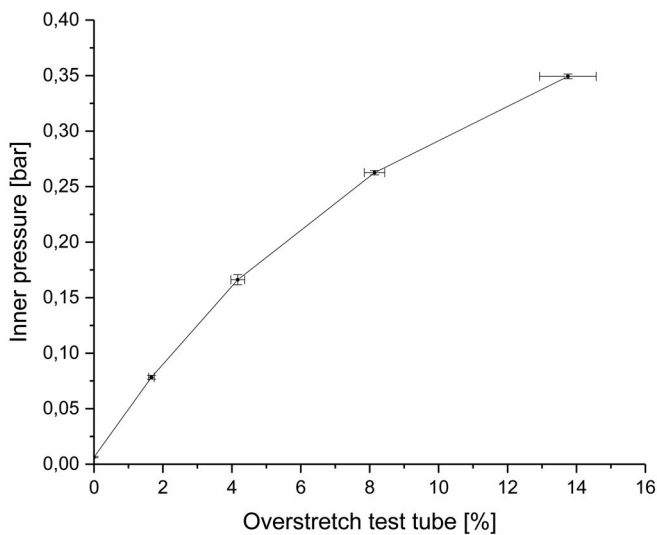**FIGURE 4** Representative images of the degrading scaffold of each group per time in the degradation test setup

FIGURE 5 Compliance measurement of the test tube (n = 5). The diameter change of the tube is presented as % overstretch

FIGURE 6 Overstretch test tube [%] per time [d] as a surrogate of the radial force loss of Res (n = 5), Res-F (n = 5), Res-P (n = 4), Res-PF (n = 4), and Mag (n = 4) in the degradation test setup

4.1 | Device surface

A duplex coating of fluoride and a polymeric layer seems to present a synergistic effect by significantly slowing degradation in an in vitro study. With this passivation combination, Res-PF is able to out-perform Magmaris in a bench test.

Magnesium fluoride, as a stand-alone passivation layer in Res-F, presents a bit of a challenge. The SEM image (Figure 2a) shows the MgF_2 surface of Res-F directly after surface modification and before any mechanical deformation by crimping or dilation. Already in this state, fine cracks are visible in the passivation layer, which appears covered by flake-like fluoride pieces (Figure 2b). In previous studies, spatial defects of inorganic coatings on metal surfaces were found to be limiting for the overall protection abilities of a passivation layer long-term.[19] For implants that undergo massive reshaping during application like scaffolds, the passivation layer is additionally weak-ened by its limited ability for plastic deformation. After crimping and dilation of Res-F, the cracked passivation layer has several fluoride flakes missing which results in an increased area of unprotected magnesium alloy backbone.
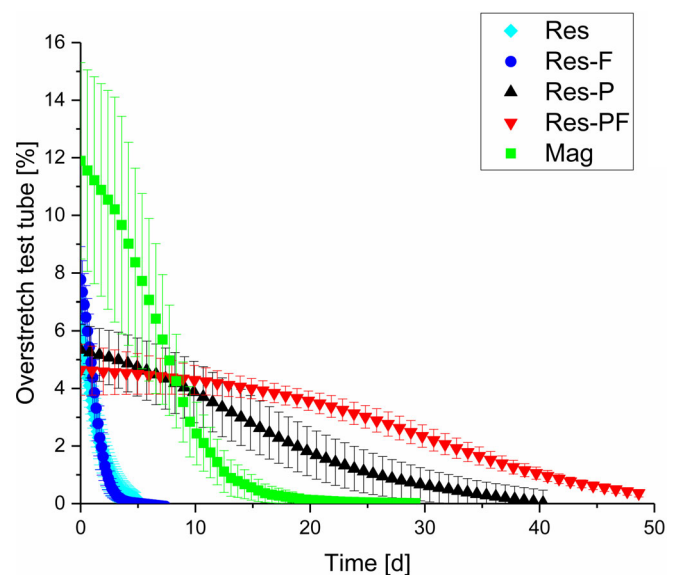
In Res-PF, the thin polymeric topcoat was able to mask the cracks in the passivation layer completely, indicating that the gateway for corrosive media to penetrate the passivation layer has been closed (Figure 2c,d). Even after dilation and crimping, the polymeric topcoat appeared intact. It can be speculated that the absence of delamination is a result of the stent design that was adapted to the properties of the components in order to avoid strong plastic deformation - even when dilating with rated burst pressure (Figure 2c).

4.2 | Degradation study

In the present experiment, the fluoride passivation layer (Res-F) resulted in only a slightly lower release of Mg^{2+} compared to an unmodified Res scaffold. The SEM images indicate that the cracks caused by the strong deformation of the brittle fluoride layer during crimping and dilation of the scaffold are very likely responsible for the lack of effective passivation. In previous reports about passivation

properties of a fluoride layer, the tests were performed on rigid samples such as discs or pins, where the brittle passivation layer was not subjected to any deformation and therefore showed better performance. The additional requirement of flexibility of a protective layer represents a further challenge, which greatly limits the use of inorganic passivation layers such as MgF_2.

Polymeric layers usually have a higher flexibility than inorganic layers and are better suited for these purposes, as seen in Figure 2c. In the current test, the polymer coating on the stent (Res-P) provided 30x better protection against a corrosive attack of PBS than a fluoride layer (Res-F). A duplex layer of fluoride and a top layer of PLLA (Res-PF) offers a type of synergistic protection and reduces the degradation 80x compared to a bare Res scaffold (Figure 3), which is more than could be expected from the results of the two individual components (Res-F and Res-P). This could be explained by the fact that the
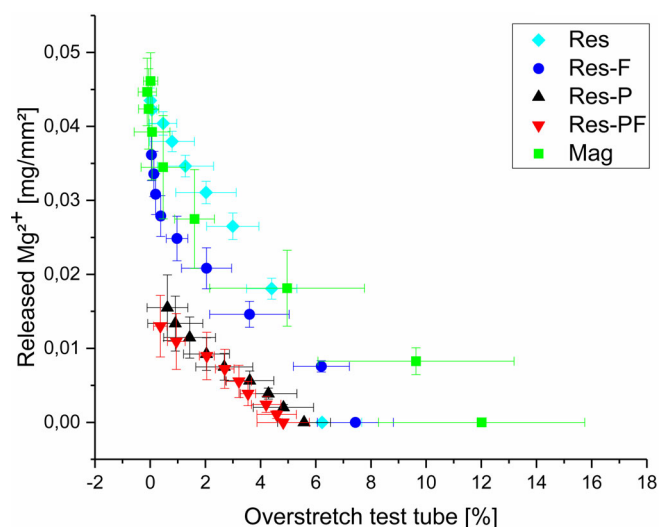

FIGURE 7 Released Mg^{2+} [mg/mm^2] per overstretch test tube [%] of Res (n = 5), Res-F (n = 5), Res-P (n = 4), Res-PF (n = 4), and Mag (n = 4) in the degradation test setup

fluoride layer is held close to the surface of the scaffold by the elastic top layer even when cracks form, and can thus still perform a protective function. In addition, cracks that are likely to develop are covered and do not extend into the polymer layer. Wang et al. demonstrated a higher adhesion force of PLLA coatings on a fluoride conversion layer of a Mg-alloy than on a polished bare Mg-alloy surface. The higher adhesion force could prevent the PLLA coating from delamination after crimping and dilation and therefore reduce the degradation rate.[20]

Both polymer-coated Resoloy scaffold modifications (Res-P and Res-PF) outperformed the Magmaris scaffold 5× and 8×, respectively. Figure 4, with photos at different stages of degradation, supports the results of the Mg^{2+} release. The Magmaris scaffold darkened significantly at the beginning of the degradation test, indicating that degradation of the Mg alloy had started. Said degradation would only be possible if water was able to diffuse through the polymer. Between day 5 and day 10, the color of the Magmaris continued to fade, indicating that the metallic backbone continued degrading. By day 20, only tiny fragments of Mg alloy were still visible within the transparent PLLA sheath. After 40 days, Magmaris dismantled completely while the two Res modifications with the PLLA layer (Res-P and Res-PF) were still present in their test tubes.

While bulk degradation (measured as Mg^{2+} release) is an important material property, information about the duration of scaffolding ability during dismantling is a more significant parameter. The scaffold will maintain its function as long as its radial support is higher than the recoil force of the target lesions. Even though the exact recoil force in a diseased coronary artery is largely unknown, the diameter change of the implant in an elastic tube with known compliance provides new information about the expected in vivo performance. The diameter measurement of an oversized tube is so far the only published method for serial assessment of the mechanical stability of scaffolds during degradation.

The loss of mechanical stability (measured by the decrease of the diameter of the overstretched test tube in Figure 6. correlated with
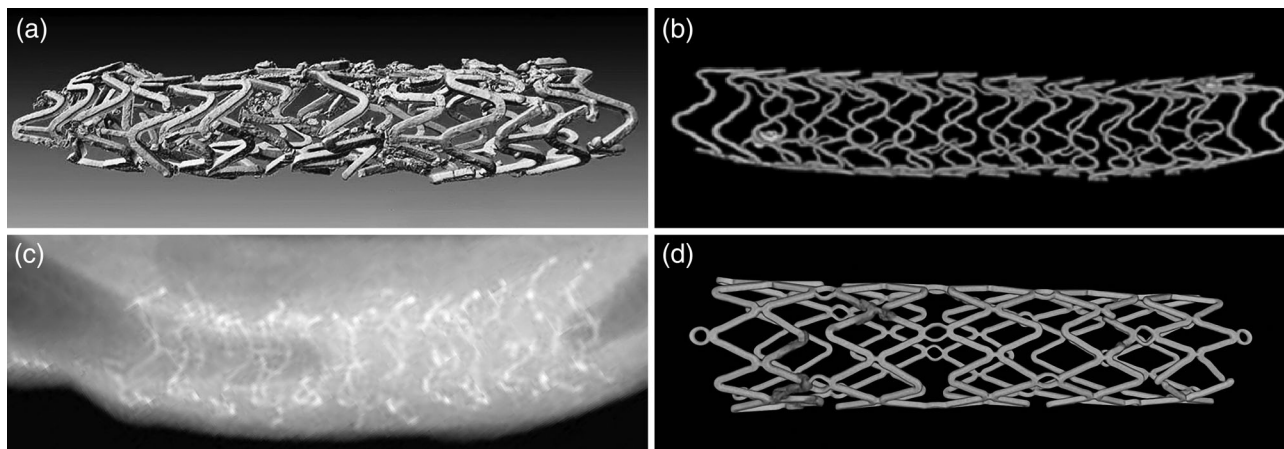

FIGURE 8 Magnesium-based resorbable scaffolds at 1 month follow up in preclinical trial: (a) Mg-Nd-Zn-Zr alloy (JDBM); μ-CT[11]; (b) Mag (Magmaris; Biotronik); μ-CT[8]; (c) WE43 scaffold without coating (Biotronik); faxitron [30]; (d) Res-PF (MeKo); μ-CT

TABLE 2 Quantitative coronary angiography, histopathology, and morphometry

Follow-up	Group (n)	Balloon to artery ratio	LLL [mm]	Mean post [mm]	Injury score	Inflamm. score	Fibrin score	Endothelial. score	Lumen area [mm^2]	Neointimal area [mm^2]	Medial area [mm^2]	EEL area [mm^2]
12 days	Res-F (3)	1.10 ± 0.04	0.04 ± 0.11	3.00 ± 0.15	0.16 ± 0.16	1.34 ± 0.36	0.74 ± 0.33	2.55 ± 0.39	6.39 ± 0.63	0.96 ± 0.15	1.24 ± 0.20	8.58 ± 0.65
	Res-PF (3)	1.15 ± 0.03	0.28 ± 0.18	3.13 ± 0.21	0.23 ± 0.14	1.75 ± 0.17	1.47 ± 0.40	2.33 ± 0.34	6.26 ± 0.58	1.36 ± 0.30	1.33 ± 0.20	8.96 ± 0.68
	p-value	0.12	0.01	0.46	0.60	0.15	0.07	0.50	0.815	0.11	0.59	0.526
28 days	Res-F (3)	1.12 ± 0.05	0.57 ± 0.22	2.88 ± 0.17	0.33 ± 0.40	1.29 ± 0.07	0.13 ± 0.07	2.89 ± 0.19	4.29 ± 0.93	1.55 ± 0.62	1.37 ± 0.38	7.20 ± 1.07
	Res-PF (3)	1.14 ± 0.04	0.41 ± 0.20	3.00 ± 0.16	0.41 ± 0.18	1.26 ± 0.21	0.28 ± 0.09	3.00 ± 0.00	4.41 ± 0.78	2.22 ± 0.35	1.29 ± 0.15	7.92 ± 0.85
	p-value	0.65	0.41	0,15	0.78	0.81	0.09	0.37	0.70	0.18	0.75	0.41

Note: Values are expressed as mean ± standard deviation.

the release of magnesium ions. However, the correlation is not proportional for all test groups and some test groups lose support somewhat faster than would be expected from the ion release results.

Figure 7 shows that the polymer-coated scaffolds (Res-P, Res-PF, Mag) exhibited a faster loss of radial strength per released Mg^{2+}, which could be explained by localized degradation due to coating defects after crimping and expansion of the scaffolds.[21] At the location of these defects, the degradation of the metallic backbone progressed more rapidly while other parts of the stent were protected, thus reducing the total amount of magnesium ions released. Despite the above-mentioned findings, it should be noted that the degradation of the polymer-coated scaffolds is still substantially slower than that of non-polymer coated scaffolds.

The Magmaris differs from the other tested scaffolds in the presence of a lipophilic drug (Sirolimus) in the coating. So far, nothing has been published about the influence of said drug on magnesium degradation in bench tests, therefore direct comparison to Res-P or Res-PF is difficult.

4.3 | Animal study

Because the in vivo degradation kinetics of Resoloy are largely unknown, an early follow up time of 12 days was chosen in addition to the classical follow up time of 28 days. This ensured that any potential early collapse in one of the test groups would be detected. Unlike the collapse of a permanent stent, the vessel narrowing in the case of a scaffold is only temporary, followed by a compensatory movement of the vessel when the stent has lost its structural integrity. In angiographic control at a later stage, vessel opening after collapse is difficult to distinguish from good performance of an intact stent. In the first preclinical studies of bioresorbable scaffolds, this behavior led to false hopes in performance.

4.3.1 | Scaffold ability

Assessing scaffolding ability in a preclinical trial can be challenging since any analysis is prone to artifacts. Only in the case that the morphometrically assessed stent area is in the range of the expected theoretical value, can one be certain of the scaffold´s structural integrity. If the scaffold area is more than 5–10% smaller than the expected value, based on the contrast media-filled balloon during implantation, it is unclear whether the known shrinkage of histological samples during tissue processing is responsible for the loss of area or if the scaffold integrity was already lost before vessel harvesting and the vessel was kept open by blood pressure. In that case, careful analysis of the postprocedural angiographic vessel diameter and morphometric neointima area of a stented vessel segment allows an assessment of whether angiographic lumen loss at follow up is more likely to be caused by proliferation or a loss of structural integrity of the implant. The present experiment is not sufficient in terms of the sample numbers to clearly prove these relationships, but researchers with a great deal

FIGURE 9 Strut cross sections from histological samples show different recognition of the CaP degradation product by macrophages: (a) Mag; energy dispersive X-ray analysis at 180d with Ca coloured in red[8]; (b) Mag; HE stain at 720d; parts of black coloured CaP fell out of the histological slide during the cutting process[8]; (c) Res-PF; HE stain at 28d; beginning macrophage infiltration

of experience in testing degradable implants can certainly identify recurring patterns.

At 12 days, the scaffolds of Res-PF and Res-F exhibited no reduction in morphometrically-assessed scaffold area. The higher angiographic area loss of Res-PF compared to Res-F was caused mainly by differing amounts of neointimal proliferation. At 28 days, the angiographic area loss of Res-F was more distinct, which was not a consequence of hyperplasia as seen in the neointima area, but most likely the result of a reduced scaffold diameter. Based on this, it can be assumed that scaffolds of Res-PF were stable at 12d and at 28d, whereas the remaining radial strength of Res-F decreased between 12d and 28d.

As the preclinical study was performed in the same lab as Biotronik's Magmaris test series, using the same animal breed, the same analytical methods and the same vessel oversizing in the regarding groups (balloon/artery ratio: 1.12–1.14), the preclinical results of the Magmaris scaffold can be used in place of a control group for the current study.[7] The LLL (Magmaris: 0.48 vs 0.41 in PF) and neointimal proliferation (Magmaris: 2,22mm^2 vs 2,20mm^2 in PF) are very similar, indicating comparable scaffold stability and preclinical efficacy at 28d. Interestingly, the Res-PF was able to achieve this goal without the use of any antiproliferative drug, which can be added in the next step of development, giving hope to further improved performance.[22]

The μ-CT and Faxitron images of different magnesium-based scaffolds from preclinical studies showed different stages of progress in degradation and loss of structural integrity after 28d (Figure 8a-d). The cylindrical shape and structural integrity of the Res-PF group support the results of the stability assessment and show the slower degradation of Res-PF in comparison to the presented scaffolds.

4.3.2 | Biological response

The addition of a bioresorbable PLLA topcoat led to a slightly slower healing process in Res-PF (fibrin score) and a higher proliferation (neointimal area) compared to Res-F, but not to increased inflammation. The vessel oversize was quite similar in both test groups resulting in a comparable injury score, and can therefore be excluded as a reason for the increased proliferation. It is well accepted that

inflammatory reaction to polymer coatings plays an important causative role in the process of delayed arterial healing after DES implantation.

4.3.3 | Degradation

Large differences in degradation kinetics resulting from the bench test decreased significantly during preclinical testing. The poor translation of in vitro degradation results to in vivo performance has been reported several times,[23] but the reason for it is still unclear. It can be speculated that, especially in the case of vascular implants, the lack of mechanical stress during degradation in the bench test model does not sufficiently address localized corrosion mechanisms such as stress crack corrosion (SCC) and corrosion fatigue (CF). In preclinical testing, degradation of scaffolds was not yet in an advanced stage when loss of support occurred.[9] It was suggested that especially SCC and CF limit the function of a scaffold in vivo[24] and are believed to be the most dangerous forms of corrosion-assisted failures.[25] In addition, the absence of proteins and cells, as well as the selected buffer solution (PBS) influences the in vitro degradation results.[23]

Of particular interest is the biological response to the degradation process of Resoloy. The area of the degraded Resoloy struts was already entered by cells after 28d (Figure 9c). This is remarkable as no cell infiltration of the strut area was reported in any of the Magmaris studies. The Magmaris CaP conversion product (Figure 9a) was still visible in histology and in OCT[7] until the last follow up time point of more than 2 years (Figure 9b), which was unexpected since CaP is known to be quickly digested in vivo[26] and in cell cultures. It has been observed that in the presence of foreign ions within the CaP matrix, phagocytosis can be influenced. Ion-substituted calcium phosphates not only have a different solubility than the undoped material, but may modify the resorption kinetic due to the release of the doping agent.[27] It can therefore be hypothesized that one or more of the alloying elements in WE43 play a decisive role for the hindered resorption of the conversion product.

Since no such finding has been reported for other magnesium alloys such as AZ31B[22] or Mg-Nd-Zn-Zr,[11,28] it can be assumed that

the modified composition of alloying elements in Resoloy could lead to potentially residue-free degradation.

Preclinical studies with longer observation times are necessary to confirm that the scaffold will be bioresorbed without formation of a permanent CaP conversion product. Further studies over 6–12 months will be conducted to shed light on the long-term performance of the Resoloy scaffolds.

5 | CONCLUSION

The in vitro degradation test shows that a combination of MgF_2 passivation and a PLLA topcoat on a Resoloy magnesium backbone leads to a much slower degradation and a longer support time than a Magmaris control group. In a preclinical study, the safety and efficacy of this duplex layer could be demonstrated. The beginning colonization of the degraded strut area by macrophages can be seen as clear indications that the resorption of the intermediate degradation product takes a different course than that of the Magmaris scaffold.

6 | STUDY LIMITATIONS

The in vitro degradation study was performed with PBS, which has a higher phosphate ion concentration than blood. It is unknown how much this influences the degradation kinetic overall, and if Resoloy and Magmaris (WE43) are affected in the same way. The degradation test is not able to mimic the complex 3D motion of the coronary arteries during the heartbeat.

A limitation of the current study is the absence of a control group in the preclinical study, caused by limited access to the Magmaris scaffold at the start of the study.

Based on the different appearance (presence of a visible polymer coating in one group) in histopathology and morphometry, it was also not possible to blind the study pathologist. The sample number was not intended to reach statistically significant group differences.

The healthy porcine coronary artery model used cannot mimic a diseased human coronary artery, but ensures a better understanding of the scaffold behavior compared to in vitro tests.

DATA AVAILABILITY STATEMENT
Data available on reasonable request from the authors

ORCID
Roman Menze https://orcid.org/0000-0001-6437-3808

REFERENCES

1. Bønaa KH, Mannsverk J, Wiseth R, et al. Drug-eluting or bare-metal stents for coronary artery disease. *New Engl. J. Med.* 2016;*375*(13): 1242-1252. https://doi.org/10.1056/NEJMoa1607991.
2. Hofma SH, Van Der Giessen WJ, Van Dalen BM, et al. Indication of long-term endothelial dysfunction after sirolimus-eluting stent implantation. *Eur Heart J.* 2006;*27*(2):166-170. https://doi.org/10.1093/eurheartj/ehi571.
3. Nakazawa G, Otsuka F, Nakano M, et al. The pathology of neo-atherosclerosis in human coronary implants: bare-metal and drug-eluting stents. *J Am Coll Cardiol.* 2011;*57*(11):1314-1322. https://doi.org/10.1016/j.jacc.2011.01.011.
4. Serruys PW, Chevalier B, Sotomi Y, et al. Comparison of an everolimus-eluting bioresorbable scaffold with an everolimus-eluting metallic stent for the treatment of coronary artery stenosis (ABSORB II): a 3 year, randomised, controlled, single-blind, multicentre clinical trial. *The Lancet.* 2016;*388*(10059):2479-2491. https://doi.org/10.1016/S0140-6736(16)32050-5.
5. Haude M, Erbel R, Erne P, et al. Safety and performance of the DRug-eluting absorbable metal scaffold (DREAMS) in patients with de novo coronary lesions: 3-year results of the prospective, multicentre, firstin-man BIOSOLVE-I trial. *EuroIntervention.* 2016;*12*(2):e160-e166. https://doi.org/10.4244/EIJ-D-15-00371.
6. Garcia-Garcia HM, Haude M, Kuku K, et al. In vivo serial invasive imaging of the second-generation drug-eluting absorbable metal scaffold (Magmaris — DREAMS 2G) in de novo coronary lesions: insights from the BIOSOLVE-II first-in-man trial. *Int J Cardiol.* 2018;*255*:22-28. https://doi.org/10.1016/j.ijcard.2017.12.053.
7. Waksman R, Zumstein P, Pritsch M, et al. Second-generation magnesium scaffold Magmaris: device design and preclinical evaluation in a porcine coronary artery model. *EuroIntervention.* 2017;*13*(4):440-449. https://doi.org/10.4244/EIJ-D-16-00915.
8. Joner M, Ruppelt P, Zumstein P, et al. Preclinical evaluation of degradation kinetics and elemental mapping of first- and second-generation bioresorbable magnesium scaffolds. *EuroIntervention.* 2018;*14*(9): e1040-e1048. https://doi.org/10.4244/eij-d-17-00708.
9. Wittchow E, Adden N, Riedmüller J, Savard C, Waksman R, Braune M. Bioresorbable drug-eluting magnesium-alloy scaffold: design and feasibility in a porcine coronary model. *EuroIntervention.* 2013;*8*(12):1441-1450. https://doi.org/10.4244/EIJV8I12A218.
10. Slottow TLP, Pakala R, Okabe T, et al. Optical coherence tomography and intravascular ultrasound imaging of bioabsorbable magnesium stent degradation in porcine coronary arteries. *Cardiovasc Revasc Med.* 2008;*9*(4):248-254. https://doi.org/10.1016/j.carrev.2008.04.001.
11. Zhang J, Li H, Wang W, et al. The degradation and transport mechanism of a mg-Nd-Zn-Zr stent in rabbit common carotid artery: a 20-month study. *Acta Biomater.* 2018;*69*:372-384. https://doi.org/10.1016/j.actbio.2018.01.018.
12. Lu P, Cao L, Liu Y, Xu X, Wu X. Evaluation of magnesium ions release, biocorrosion, and hemocompatibility of MAO/PLLA-modified magnesium alloy WE42. *J Biomed Mater Res—Part B Appl Biomater.* 2011;*96 B*(1):101-109. https://doi.org/10.1002/jbm.b.31744.
13. Zhang D, Qi Z, Shen H, Wei B, Zhang Y, Wang Z. In vitro degradation and cytocompatibility of magnesium alloy coated with Hf/PLLA duplex coating. *Mater Lett.* 2018;*213*:249-252. https://doi.org/10.1016/j.matlet.2017.11.080.
14. Oliver JJ, Webb DJ. Noninvasive assessment of arterial stiffness and risk of atherosclerotic events. *Arterioscler Thromb Vasc Biol.* 2003;*23*(4):554-566. https://doi.org/10.1161/01.ATV.0000060460.52916.D6.
15. Chagnon M, Guy LG, Jackson N. Evaluation of magnesium-based medical devices in preclinical studies: challenges and points to

consider. *Toxicol Pathol*. 2019;47:390-400. https://doi.org/10.1177/0192623318816936.

16. Hopkins C, Sweeney CA, O'Connor C, McHugh PE, McGarry JP. Webbing and delamination of drug eluting stent coatings. *Ann Biomed Eng*. 2016;44(2):419-431. https://doi.org/10.1007/s10439-015-1490-5.

17. Nakatani S, Yamagishi M, Tamai J, et al. Assessment of coronary artery distensibility by intravascular ultrasound. *Circulation*. 1995;91 (12):2904-2910. https://doi.org/10.1161/01.CIR.91.12.2904.

18. Shimazu T, Hori M, Mishima M, et al. Clinical assessment of elastic properties of large coronary arteries: pressure-diameter relationship and dynamic incremental elastic modulus. *Int J Cardiol*. 1986;13(1): 27-45. https://doi.org/10.1016/0167-5273(86)90077-X.

19. Merl DK, Panjan P, Panjan M, Čekada M. The role of surface defects density on corrosion resistance of PVD hard coatings. *Plasma Processes Polym*. 2007;4:613-617. https://doi.org/10.1002/ppap.200731416.

20. Wang Z, Guo Y. Corrosion resistance and adhesion of poly(L-lactic acid)/MgF2 composite coating on AZ31 magnesium alloy for biomedical application. *Russ J Non-Ferrous Metals*. 2016;57(4):381-388. https://doi.org/10.3103/S1067821216040155.

21. Maier P, Steinacker A, Clausius B, Hort N. Influence of solution heat treatment on the microstructure, hardness and stress corrosion behavior of extruded Resoloy®. *JOM*. 2020;72(5):1870-1879. https://doi.org/10.1007/s11837-020-04077-9.

22. Li H, Zhong H, Xu K, et al. Enhanced efficacy of Sirolimus-eluting bioabsorbable magnesium alloy stents in the prevention of restenosis. *J Endovasc Ther*. 2011;18(3):407-415. https://doi.org/10.1583/10-3353.1.

23. Gonzalez J, Hou RQ, Nidadavolu EPS, Willumeit-Römer R, Feyerabend F. Magnesium degradation under physiological conditions – best practice. *Bioactive Mater*. 2018;3(2):174-185. https://doi.org/10.1016/j.bioactmat.2018.01.003.

24. Jafari S, Harandi SE, Singh Raman RK. A review of stress-corrosion cracking and corrosion fatigue of magnesium alloys for biodegradable implant applications. *JOM*. 2015;67(5):1143-1153. https://doi.org/10.1007/s11837-015-1366-z.

25. Harandi SE, Singh Raman RK. Appropriate corrosion-fatigue testing of magnesium alloys for temporary bioimplant applications. *Magnesium Technol*. 2016;353-356. https://doi.org/10.1007/978-3-319-48114-2_68.

26. Frayssinet P, Gineste L, Conte P, Fages J, Rouquet N. Short-term implantation effects of a DCPD-based calcium phosphate cement. *Biomaterials*. 1998;19(11–12):971-977. https://doi.org/10.1016/S0142-9612(97)00163-4.

27. Boanini E, Gazzano M, Bigi A. Ionic substitutions in calcium phosphates synthesized at low temperature. *Acta Biomater*. 2010;6(6): 1882-1894. https://doi.org/10.1016/j.actbio.2009.12.041.

28. Zhang J, Hiromoto S, Yamazaki T, et al. Macrophage phagocytosis of biomedical mg alloy degradation products prepared by electrochemical method. *Mater. Sci. Eng. C*. 2017;75:1178-1183. https://doi.org/10.1016/j.msec.2017.02.126.